Journal of *Marine Science and Engineering*

MDPI

Article

Waves as Energy Source for Desalination Plants in Islands

B. Del Río-Gamero *, Ancor José Yánez-Rivero, P. Yánez Rosales and Julieta Schallenberg-Rodríguez

Process Engineering Department, Industrial and Civil Engineering School, Universidad de Las Palmas de Gran Canaria, 35017 Las Palmas de Gran Canaria, Spain; ancor.yanez101@alu.ulpgc.es (A.J.Y.-R.); pablo.yanez@ulpgc.es (P.Y.R.); julieta.schallenberg@ulpgc.es (J.S.-R.)
* Correspondence: beatriz.delrio@ulpgc.es

Abstract

The rapid increase in the global demand for electricity and the resulting emission of polluting gases, together with the limited availability of land suitable for renewable energy installations in some areas, are the motivation for this study. The Canary Islands, characterized by rugged terrain and limited water resources, provide the context for this research in which the interconnection between water and energy is the central focus. This work examines the technical viability of meeting the annual energy requirements of island-based desalination facilities by wave energy, with the objective of diminishing dependence on fossil fuels and ensuring the water supply. Five wave energy converters were compared under three scenarios with increasing levels of constraints, including single-device installations and wave farm configurations. The first scenario evaluated the unit performance of each device, showing WaveStar to be the most operationally robust option. The second and third scenarios shifted the analysis to a wave farm layout with and without environmental restrictions. The results showed that Wave Dragon and WaveStar farms achieve the highest production levels and best installed power densities. Each offers different advantages, with Wave Dragon concentrating high power in a few units and WaveStar presenting greater modularity and better resistance to adverse conditions.

Keywords: wave energy; desalination; Canary Islands; renewable energy; replicability

check for updates

Academic Editor: Dominic E. Reeve

Received: 5 November 2025
Revised: 29 November 2025
Accepted: 2 December 2025
Published: 6 December 2025

Citation: Río-Gamero, B.D.; Yánez-Rivero, A.J.; Yánez Rosales, P.; Schallenberg-Rodríguez, J. Waves as Energy Source for Desalination Plants in Islands. *J. Mar. Sci. Eng.* **2025**, *13*, 2320. https://doi.org/10.3390/jmse13122320

1. Introduction

Water stress, a global challenge affecting ecosystems, economies and millions of people around the world, has transformed the way we manage one of the most essential resources for life. One of the technological responses to the problems caused by water stress has been the increasing deployment of desalination. Currently, 300 million people meet their water needs by converting saline water into water suitable for consumption [1]. Desalination has consolidated its position as a key solution in more than 150 countries, where currently some 18,000 plants operate with an installed capacity of about 95 million cubic meters per day [1,2].

Among the several technologies used to desalinate water, reverse osmosis (RO) is the market leader with over 69% of the global share thanks to its lower specific energy consumption (2–4 $kWh \cdot m^{-3}$) [3]. Taking into account all the technologies employed and their share in total production, the global energy consumption for desalination ranges between 189 and 331 TWh/year [4]. This value represents between 0.7% and 1% of worldwide global electricity consumption which amounted to 29,000 TWh in 2023 [5]. The main problem with this energy consumption is the source used to produce it. In this regard, 45% of gross electricity consumption in Europe is covered by renewable energy (RE), but this value can vary

considerably between countries and indeed between regions within the same country [6]. In Spain, for example, the emission of greenhouse gases differs considerably between the Iberian Peninsula and the Canary Islands, as the energy mix in the islands is much more dependent on fossil fuels. Worldwide, and with respect to desalination specifically, indirect emissions associated with this technology as it is presently being deployed could be as high as 400 million tons by 2050 [1,7]. As a consequence of the growing awareness of the desalination energy consumption problem, this is the second most covered research area in the desalination sector, with 28% of publications in the last five years contributing to this topic [8,9]. At the industrial level, less than 1% of desalination plants use RE as their main source [10,11], with solar photovoltaic (PV) technology leading in terms of installation percentage (32%), followed by wind (19%) and solar thermal (13%) [12–14].

Increasing the penetration of RE not only reduces greenhouse gas emissions, but also promotes energy self-sufficiency by using locally available renewable resources [15]. In economic terms, once the initial investment has been recouped, the operating cost associated with the use of RE is lower than that of conventional systems, particularly in locations with high renewable resources. Furthermore, there is a convergence between water scarcity and renewable resources, in that in many regions with water stress there is high solar, wind or wave power potential [16]. This is particularly important in remote, isolated areas or areas far from the electricity grid, as it allows for the implementation of decentralized solutions that improve access to drinking water without requiring extensive infrastructure [17].

The main disadvantage of renewable sources is that they are subject to daily and seasonal variability [18], which affects the continuous operation of the plant if there is no energy storage or backup system through technological hybridization. In addition, the implementation of PV, wind or solar thermal systems with sufficient capacity to power a desalination plant involves considerable capital expenditure [19], which can be a barrier in contexts with limited funding. In addition, such systems also require a significant surface area for deployment and operation [20]. Finally, some thermal desalination technologies, such as multi-stage flash distillation, cannot be easily adapted to the intermittent nature of renewable sources [21]. Figure 1 shows a summary of the main advantages and disadvantages of the integration of RE technologies in desalination systems.

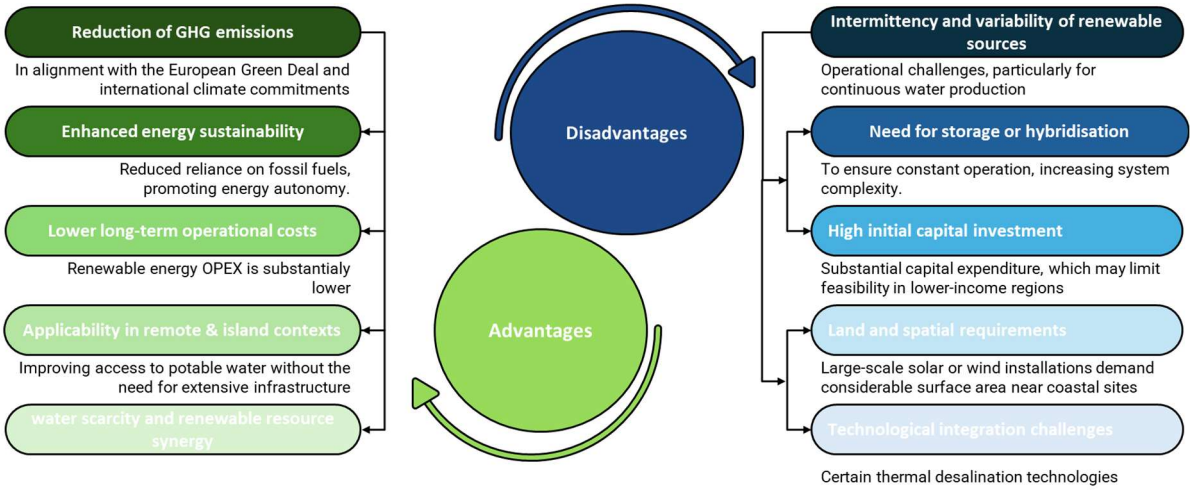

Figure 1. Advantages and disadvantages of integrating renewable energy technologies into desalination systems.

The fluctuation and intermittency of RE sources present pressing technical and economic challenges that have proven an obstacle to the deployment of large-scale commercial

RO plants [22]. However, this barrier can be overcome thanks to ocean wave energy. This technology offers a renewable resource with the advantage of being predictable several days in advance, consistent throughout the day and night, and with a significantly higher energy density compared to wind and solar [23]. Additionally, the natural geographical coincidence with the location of desalination plants, generally in coastal areas, contributes to reducing energy transport losses and simplifying infrastructure requirements [24]. Furthermore, wave energy installations do not occupy land or generate significant visual impacts, which is very important, especially in territories where land is limited and there is competitive use of it, as in the case of islands [25].

In the Canary Islands, approximately 80% of potable water is obtained through desalination [26]. This activity, which is almost entirely powered by fossil fuels, emits around 2.8 kg CO_2 m^{-3} [27], with an annual consumption of around 4.5 TWh [28]. Powering these desalination complexes with fossil fuels exacerbates the environmental impact of desalination. It increases emissions associated with the process and reinforces dependence on a type of energy that is highly volatile economically. Furthermore, the electricity required for the process accounts for around 44% of the final cost of the desalinated water [29]. This combination of factors limits the sustainability of the model. For all these reasons, the Canary Islands archipelago was selected as a case study in the use of wave energy as an energy source for desalination plants.

The primary objective of the present study is to assess the potential for the integration of different wave energy converters in different scenarios in order to meet the energy demand of public desalination plants in the Canary Islands. Several specific objectives were established that integrate each phase of the study, including an analysis of the geographical and marine characteristics of the Canary Islands, which are key to the deployment of a new renewable technology that is currently maturing. Simulation of various wave energy converters (to see which operating principles could be adapted to the particular circumstances of the Canary Islands), constitutes another of the specific objectives.

This approach contributes to improving future strategic planning for sustainable infrastructure in the archipelago. The stability of wave energy as a marine resource facilitates its direct connection to the desalination plant, with little reliance on batteries or the grid. At the same time, it would alleviate the burden on the Canary Islands' electricity grids, especially when a future increase in energy demand is expected due to the electrification of transport. Ensuring access to drinking water strengthens essential activities such as agriculture, tourism and industry, reinforcing the economic development of the Canary Islands.

Several studies have been conducted to independently assess the wave resources of the seven Canary Islands, such as the work of G. Iglesias and R. Carballo for the islands of La Palma and El Hierro [30,31], J.P. Sierra et al. advising the island of Lanzarote [32] and M. Veigas et al. with Tenerife [33]. However, studies often use different forcing-databases (HYPOCAS, WANA, NECP, NCAR), and the spacing resolution often differs, and area restrictions are not taken into account. Veigas et al. [33] also identified it as a requirement. These gaps have been attempted to be analysed by this research group [34,35], where, in addition, this study presents a novel application in the coupling of this marine technology with desalination plants throughout the archipelago as a whole.

The novelty of this study is relevant to sustainable development by addressing multiple constraints simultaneously. It offers a practical pathway for islands with limited land availability to increase their clean-energy capacity without occupying additional terrestrial space. By integrating wave energy with desalination needs, the approach directly addresses two critical Sustainable Development Goals: ensuring access to clean water and expanding renewable energy generation [36]. It also enhances energy security, diversifies the renewable energy mix and promotes long-term resilience by reducing dependence on

fossil fuels and minimizing environmental pressures, preserving the territorial integrity of small island environments.

2. Materials and Methods

This section provides a comprehensive description of the technical methodology used to assess the potential for integrating different wave energy converters in different scenarios in order to meet the energy demand of public desalination plants in the Canary Islands.

The first scenario compares the performance of different wave energy technologies in environments close to desalination plants, defined as Scenario 1 of the study. Scenario 2 considers the maximum wave energy potential, developing the configuration of farms for the different technologies in the available areas and applying a safety distance restriction of 1.5 km from the coast. Finally, in Scenario 3, the area constraints obtained through an environmental impact study are applied. As a guide, Figure 2 shows a flow chart illustrating all the steps taken to develop the scenarios described above.

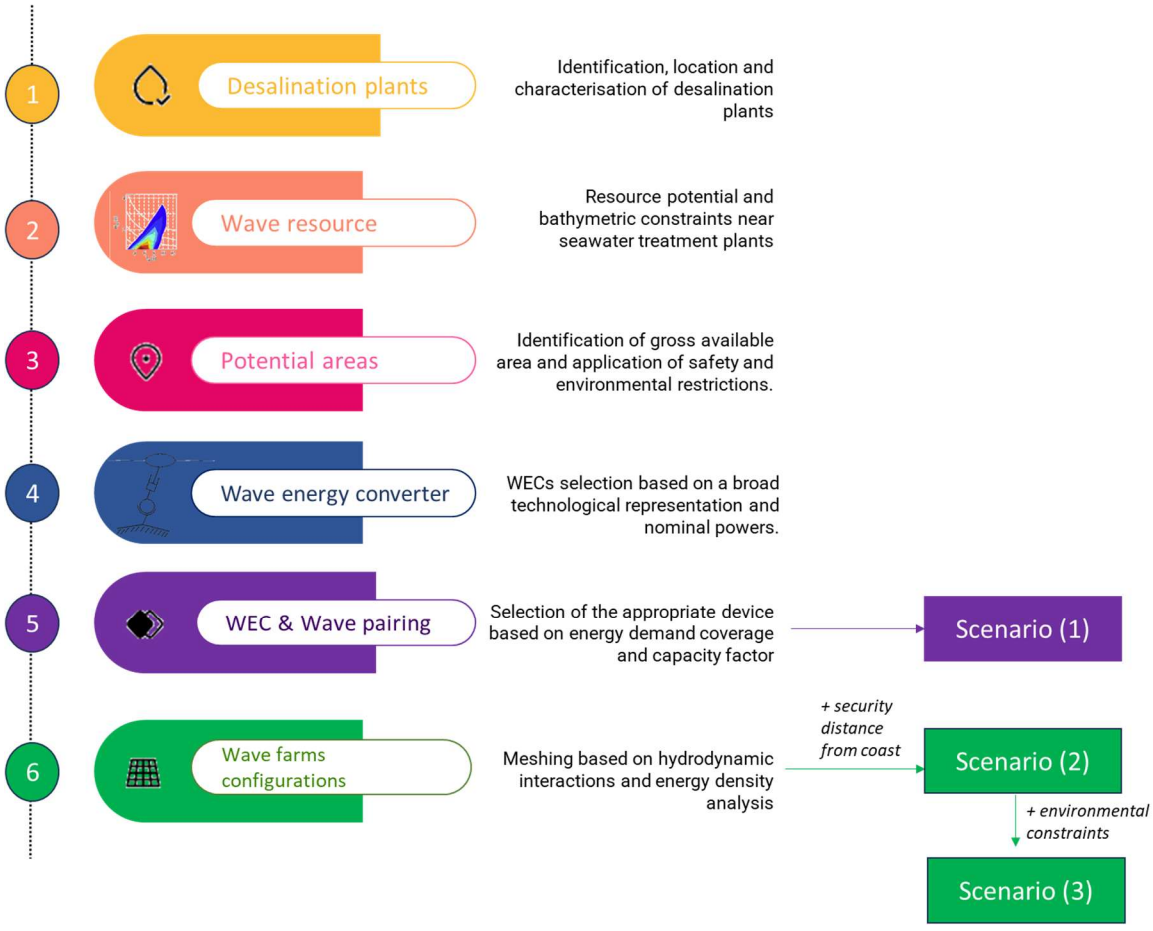

Figure 2. Methodological steps. Flow chart of the framework for evaluating the energy production of wave energy farms in order to select pairs of farms and locations.

2.1. Step 1: Identification of Desalinated Water Production Centers

Table 1 shows the different seawater desalination plants (SWDPs) to be analyzed. They are classified by island and include data on their nominal capacity and specific energy consumption. The data were obtained from scientific articles [37] and the various public and private institutions that manage and supply the plants themselves, including Canal Gestion Lanzarote [38] and ELMASA [39]. Various public documents, such as

the island water management plans [40–43], were also consulted, and some personal interviews conducted [44].

Table 1. Canary Islands desalination plants characterization.

Seawater Desalination Plant	Municipality	Nominal Capacity (m^3/d)	Specific Energy Consumption (kWh/m^3)
Lanzarote island			
Diaz Rijo	Arrecife	58,000	3.16
Janubio	Yaiza	9500	3.5
Fuerteventura island			
Puerto del Rosario	Pto. Rosario	36,500	3.5
Morrojable	Morrojable	4400	3.5
Corralejo	La oliva	12,400	3.04
Gran Tarajal	Gran Tarajal	5000	4.4
El Hierro island			
El Golfo	Frontera	1350	3.05
La Restinga	El Pinar	1700	3.18
Los Cangrejos	Valverde	2400	3.04
Gran Canaria island			
Arucas-Moya I	Arucas	15,000	3.5
Guía	Roque Prieto	10,000	3.18
Gáldar	Bocabarranco	10,000	3.5
Ayto. San Nicolás	La Aldea	10,400	3.04
Mogán	Mogán	1800	2.5
Puerto Rico	Puerto Rico	8000	3.04
Las Palmas III & IV	Jinámar	80,000	3.33
Maspalomas I & II	San Agustín	39,700	3.21
Sureste III	Pozo Izquierdo	30,000	3.5
Salinetas	Salinetas	16,000	3.5
Tenerife island			
UTE Tenerife Oeste	Fonsalía	14,000	2.16
UTE Desalinizadora de Granadilla	Granadilla de Abona	14,000	3.04
Adeje Arona	Arona	30,000	3.04
Santa Cruz I	Santa Cruz	20,000	3.04
La Caleta	Adeje	20,000	3.04

The plants were then georeferenced using the QGIS geographic information system (version 3.38.0) [44], enabling the data to be cross-referenced with the various environmental restrictions and wave resources. The database used for this purpose was the Cartográfica de Canarias (GRAFCAN) [45]. Figure 3 shows a map of the Canary Islands with the location of the desalinated water production centers and potential areas for wave energy deployment in a bathymetric range of 30–50 m.

2.2. Step 2: Wave Resource Data Acquisition and Processing

As the case study involves an entire archipelago, the assessment of the wave energy resource included a variety of coastal areas with very diverse maritime conditions. The data selection process is fundamental for this type of assessment. Long-term data series of over 20 years are highly recommended for interannual analyses. In the case of research covering large coastal areas, the use of real data from buoys is extremely complicated, so satellite data or resource maps can be consulted when looking for wave-related data series [33,46]. In the Canary Islands the longest and most extensive hindcasted data series of wave parameters is provided by the Spanish Ports Authority [47]. Known as SIMAR points, they are modelled data, with a frequency of 1 h, available for a 61-year interval up to 2025. A buoy network called REDCOS, which includes several buoys with the same hourly

data frequency, was used to validate the model [48]. Many methods have been developed to assess the resource for different accuracy levels [49,50]. In wave renewable-based studies, the most commonly used representation is a table generally referred to as the sea state diagram or sea state Scatter Diagram (SD), as reported in wave renewable reviews [9,43] (alternatively called the scatter table or joint-probability diagram [51]). Indeed, according to the above-cited studies and reviews, the SD is similar to the power matrix, a 2D table based on statistical wave height and spectral wave period parameters. For each cell of the matrix, the SD provides the frequency of occurrence of the sea-state Time Series (TS) falling within the cell's ranges of wave height and period [52]. In a previous study conducted by the authors comparing the use of TS versus SD, it was confirmed that SD (easier to use and less computationally time consuming than TS) appears to be a useful and accurate metric for annual energy production calculation [53].

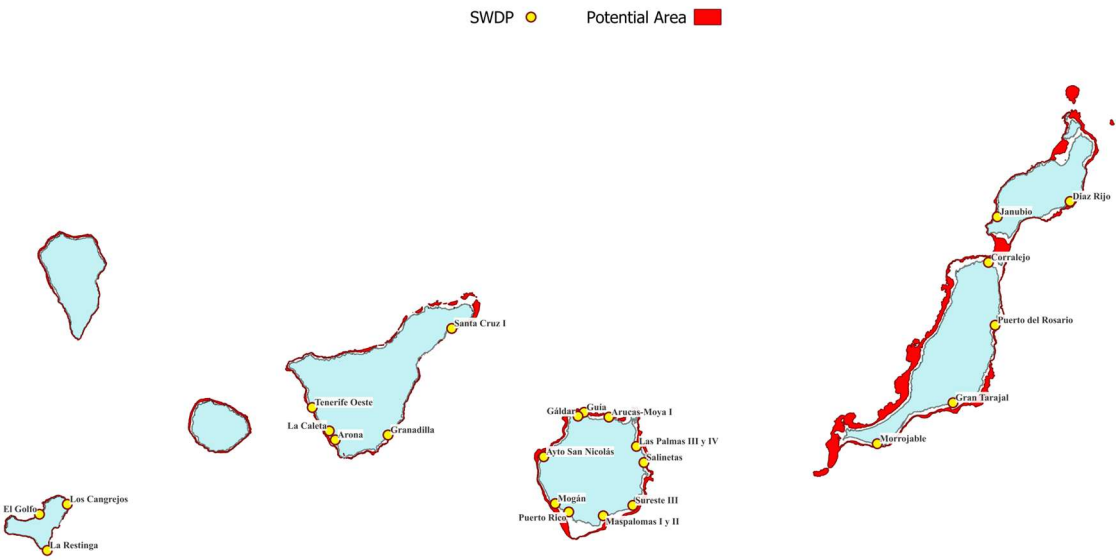

Figure 3. Map of the Canary Islands identifying seawater desalination plants (SWDP) and potential areas for wave energy deployment in a bathymetric range of 30–50 m.

The dataset was analyzed to evaluate the wave resource and obtain scatter diagrams, with calculations made of the seasonal wave direction frequency and wave power flux. The scatter diagrams show the joint distribution of significant wave height (Hs, (m)) and peak period (Tp, (s)) frequencies, statistically describing the different sea states that occur at each average location on an annual basis [54]. The selection of the different SIMAR points used was based on their proximity to the location of the various SWDPs.

2.3. Step 3: Potential Areas for Wave Energy Deployment and Environmental Constraints

The delimitation of potential areas was performed using QGIS. Based on bathymetric cartography, the −30 m and −50 m isobath curves around each island were plotted (the range coinciding with the operating depth of the selected wave converters). The result was a continuous polygon representing the gross potential area around the islands.

In order to perform operations on bathymetry maps, they must be in vector format. However, these maps are usually in raster format, so contour lines must be created using bathymetric isolines from the shadow map. To this end, a bathymetric interval of 5 m by 5 m was assumed. Once the bathymetric map is in vector format, simply select the bathymetric lines to generate the polygon between them.

Figure 4 illustrates the bathymetric map of Gran Canaria and the selection of two bathymetric limits (−30 and −50 m). However, an in-depth study of each area is required in order to define the areas of anchoring and optimal operation of the devices in detail.

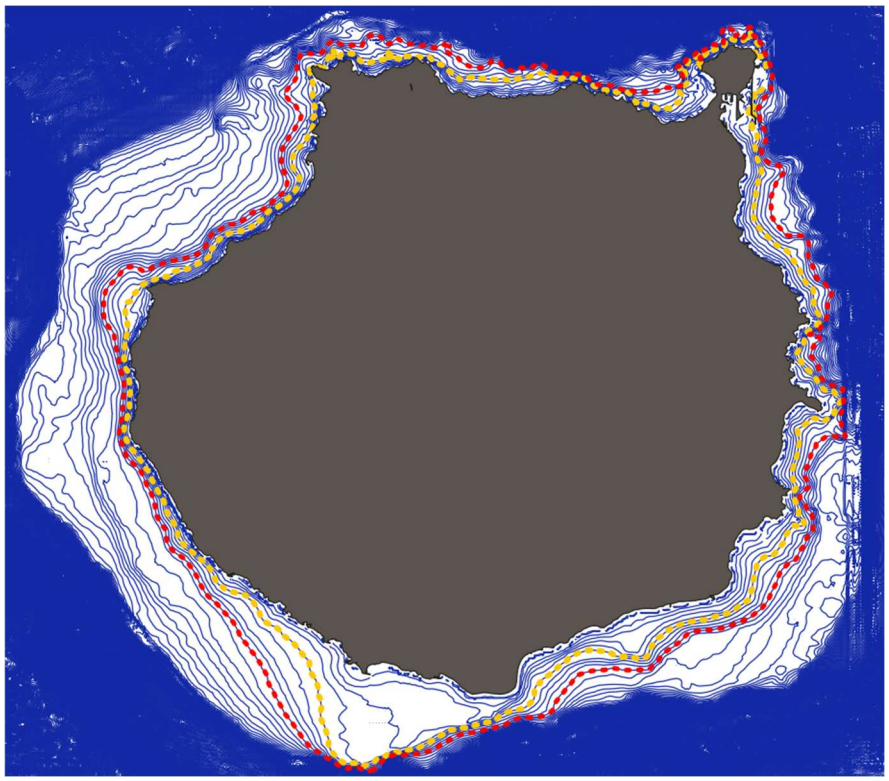

Figure 4. Bathymetric map of the Gran Canaria island, based on cartography published by the European Marine Observation and Data Network (EMODnet) [55]. Bathymetric lines every 5 m of depth (blue), −30 m bathymetric limit (yellow) and −50 m bathymetric limit (red).

Superimposed on this area were circles with a radius of 5 km focused on each SWDP, restricting the analysis to areas suitable for possible installation and defining the potential areas used in this study (Scenario 2 surface area). As a safety measure, an exclusion zone of 1.5 km was established along the coastline.

Once all the potential areas had been identified, the next step was to verify the actual availability of maritime space from an environmental and marine-use compatibility perspective. Table 2 lists all the restrictions that are used to determine potential areas for wave farms.

Table 2. Main restrictions considered to determine potential areas for waves farms.

Constraint	Shape Year	Reference
Environmental restrictions		
NATURA 2000 Special Protection Areas for birds (SPAs) Special Areas of Conservation (SAC) Sites of Community Importance (SCI)	2020	[56]
Marine Reserves	2019	[57]
Protected Natural Areas (PNAs)	2020	[58]
National Parks	2020	[59]
Infrastructure restrictions		
Fishing activities areas	2020	[60]
Navigation corridors	2023	[61]
Industrial parks and port access routes	2021	[62]
Buoys	2020	[62]
Marine cables	2020	[62]

Regarding environmental restrictions, both regional, national and international restrictions have been taken into account. At the continental level, Natura 2000 is the most significant ecological network for environmental protection. This network consists of three types of protection: Special Protection Areas (SPAs) for birds, Special Areas of Conservation (SACs) and Sites of Community Importance (SCIs). All of these areas have been excluded from the potential zones. National protected areas, such as national parks, have also been incorporated, as have local protected areas corresponding to marine reserves and Protected Natural Areas (PNAs). Information on all these protected areas can be found on the main websites of the governments of each region. Other relevant protection areas such as biosphere reserves and geoparks were not included among the constraints. Firstly, due to their potential compatibility with wave energy exploitation as their objectives often include the sustainable use of natural heritage or the prevention of climate change, and secondly because wave farms are not considered to have a significant impact on them.

The rest of the restrictions are related to human-developed marine infrastructure. These mainly refer to areas near ports, where a 1000 m safety buffer has been incorporated; marine buoys, where a 100 m buffer has been incorporated around these devices; aquaculture facilities and areas reserved for fishing, commercial shipping routes and marine cables located on the seabed, where a 100 m and 200 m buffer has been incorporated, respectively. As these last two layers have not been published by official bodies, the assumptions made by P. Yánez-Rosales et al. [62] have been used instead.

In order to apply all these constraints, the layers must first be loaded into the Geographic Information Systems (QGIS) program in vector format for further processing. This software uses multiple tools to define the difference between the potential surface layer and the restriction layers, resulting in the potential areas for wave energy development.

These restrictions have been applied in numerous studies on the zoning of marine power generation facilities, such as offshore wind farms [62–65], floating photovoltaic farms [66–68] and wave farms [34]. However, these restrictions had never previously been applied based on the technical characteristics of the wave energy devices analyzed. The main differences with these studies lie in the environmental restrictions (since wave energy devices do not pose serious problems for birds a priori), as well as the restrictions on easements and restricted areas (wave energy devices are not built to great heights).

2.4. Step 4: Wave Energy Converter Selection

Five wave energy converters (WECs) were selected for analysis based on a broad technological representation approach. To this end, systems with different operating principles, as well as with various strategies for capturing and converting wave energy, were included. Likewise, a wide range of nominal powers and designs for several wave profiles were considered. In addition, priority was given to those converters with the highest technology readiness level, incorporating those in advanced stages of development or that have already undergone testing and operational validation. More specifically, devices were included that are currently undergoing research or testing related to the scientific and industrial sector in the Canary Islands, allowing local synergies to be exploited and the results to be contextualized in a real application environment. Table 3 lists the selected converters and their key characteristics.

The three wave-energy solutions considered in this study represent distinct energy-capture mechanisms. The WaveDragon terminator extracts energy through wave overtopping into an elevated reservoir that drives low-head turbines. The OWSC devices (Langlee, PCECO) convert the horizontal surge motion of nearshore waves into rotation around a seabed-hinged flap. In contrast, point-absorber systems (Wavestar, CorPower) operate in

heave, harnessing the vertical motion of a buoy through a power-take-off system. A general characterisation of the three variants analysed can be seen in Table 4.

Table 3. Selected wave energy converters (WEC) and their key features [69–75].

WEC	Device Area (m^2)	Relevant Dimension (m)	Nominal Power (kW)	Classification	Operating Depth (m)
WaveDragon	13,000	260	5900	Terminator	30–50
WaveStar	555	12	600	Point absorber	30–50
CorPower	79	9	750	Point absorber	>30
Langlee	1500	9.5	1665	OWSC	>30
PCECO	530	9	480	OWSC	10–50

OWSC: Oscillating Wave Surge Converter.

Table 4. Technical characteristics of the three-wave energy variant solutions considered (adapted from: [53,76]).

Parameter	Variant 1. Terminator (WaveDragon)	Variant 2. Oscillating Wave Surge Converter (OWSC: Langlee/PCECO)	Variant 3. Point Absorber (Wavestar/CorPower)
Technology type	Overtopping terminator	Hinged-flap surge device	Heaving point absorber
Operation principle	Overtopping of incoming waves into a reservoir driving low-head turbines	Horizontal back-and-forth rotation of a flap driven by surge motion	Vertical heave motion converted to power via PTO
Best suited environment	High-energy wave climates	Nearshore areas with strong surge motion	Deep to intermediate waters
Bathymetry sensitivity	Moderate (requires uniform depth for stable overtopping)	High (performance strongly depends on local seabed slope)	Low-to-moderate
Spatial footprint	Large spacing due to footprint and wake effects (300–500 m)	Medium spacing (150–250 m)	Small-to-medium spacing (100–200 m)
Anchoring/ foundation	Floating structure with mooring lines	Seabed-hinged foundation	Mooring lines to seabed
Outline	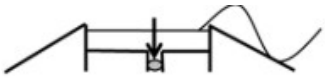	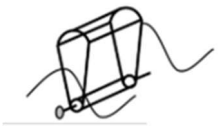	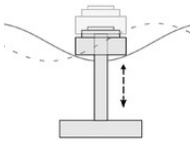

2.5. Step 5: Individual Wave Energy Converter Selection by Wave Resource Pairing

Based on the energy demand data obtained for the SWDPs and the wave resource profile in each area, the appropriate device was selected based on the energy demand coverage equivalent hours (EH) and the capacity factor (CF). EH is defined as the theoretical number of hours during which the device would operate at full capacity and CF shows the ratio between the effective annual energy production (AEP) and the energy produced if this WEC were working at its maximum capacity all year long.

Energy production was calculated combining the power matrixes of each WEC provided by the technology developers (which relate power generation to a given sea state condition as defined by Hs and Tp) with the site wave-SD (Hs–Tp distribution). Each sea state in the scatter diagram was assigned to its corresponding bin in the power matrix using the central values of significant wave height (Hs) and peak period (Tp). For each bin, the power output provided by the manufacturer was multiplied by the annual probability of occurrence of that sea state. The annual energy production was then computed as the sum of the contributions of all bins [77].

Sea states falling outside the operational range of the power matrix were assigned a power value of zero. Extremely rare sea states (with an occurrence lower than 0.1%) were retained in the calculation, but their contribution to energy production was negligible and did not affect the final results. When neighbouring matrix bins showed discontinuities, linear interpolation between adjacent Hs–Tp cells was applied to ensure numerical consistency.

Uncertainty was addressed through a sensitivity analysis in which both Hs and Tp were varied by ±10%, following common procedures in wave-energy resource assessments. This allowed evaluating the influence of measurement variability and power-matrix discretization on the resulting annual energy production. The resulting uncertainty range ±10% for Hs and ±5–10% for Tp was obtained, which is consistent with Holthuijsen [78], García-Medina et al. [79], Reguero et al. [80] and IECTS 62600-101 [81].

To quantify the energy contribution, the annual energy produced was compared with the annual electricity consumption of the SWDP. As the demand for these facilities remains relatively constant throughout the year (ignoring brief periods of downtime for maintenance, which are considered negligible), the ratio between the energy produced and the annual demand, multiplied by 100, provides the percentage of energy coverage that the converter could achieve in that area. These calculations constitute what is called Scenario 1 in the present study.

2.6. Step 6: Wave Farm Configurations

This section addresses the configuration of wave energy farms whose purpose is to fully cover the annual energy demand of each SWDP in two scenarios: the first with a safety restriction of a distance of 1.5 km from the coast (Scenario 2) and the second with the additional application of all environmental constraints (Scenario 3). An assessment of the type of technology that best suits the available area in both scenarios is then obtained from the energy density delivered by the different wave farms.

The key factors are the hydrodynamic interactions of the WECs, both in terms of near-field and far-field effects [82]. An earlier publication by the authors [22] provided a detailed timeline of these investigations, including the software packages employed to validate their methodologies. The most frequently utilized programs are NEMOH for near-field analysis, and OceanWave3D and MildWave for addressing far-field effects. These two distinct types of modeling tools have also been combined to study both interaction effects concurrently. Furthermore, the latest research efforts have successfully integrated the modeling of both phenomena simultaneously [83]. A consistent finding across all these studies is that the second row of devices captures less energy than the first row. However, only a limited number of studies specify the necessary distance to completely regenerate the wave energy, or quantify the percentage of energy reaching the second row, which is essential for optimizing the wave farm's layout [84–86]. Consequently, most authors do not provide an estimate for the optimal spacing between WECs.

In line with this, Babarit [87] introduced design guidelines for WEC arrays, which confirmed that configurations employing the minimum number of rows yield the best performance. Following this principle, Child et al. demonstrated that a staggered arrangement of the farm is superior to an aligned layout in terms of power absorption [88]. Regarding the lateral spacing between WECs within a row, increasing this distance leads to a higher energy capture rate. Nonetheless, this maximum capture rate is often not economically optimal; this trade-off is mitigated by utilizing a staggered distribution. Overall, the recommended minimum lateral separation is double the width of the WEC unit. Concerning the longitudinal distance (row-to-row separation), it varies significantly. De Andrés et al. [89] and Bozzi et al. [90] conducted research on array configurations in realistic sea conditions, concluding that the direction of the incoming waves, in addition to the WEC spacing, must

be considered during array setup. Nevertheless, these recent studies examined wave farms comprising a maximum of only four WECs and highlighted the need for more extensive studies on large-scale wave farms. A greater number of WECs was investigated by M. Giassi et al. [90], who developed a genetic algorithm-based optimization model for large-scale wave farms, but this model was restricted to farms consisting solely of point absorber Power WECs. Ultimately, all these recommendations were taken into account, and therefore the lateral and longitudinal distances between WECs were chosen based on the technical specifications and guidelines provided by the WEC manufacturers. This approach ensured the technical viability and safety of the farms and guaranteed a Q-factor (defined as the ratio of the output power of an N-unit array to the output power of N isolated units [91]) very close to 1.

Furthermore, in regions with well-defined prevailing wind directions, such as the Canary Islands, incorrect angular alignment of these devices can impact energy efficiency by between 15% and 40%, as evidenced by recent numerical and experimental models [92,93].

To this end, a calculation process was developed supported by the design of a Python script (version 3.12) [94], an open-source programming language that allows calculations to be automated and data to be visualized quickly, in order to obtain visual validation of the rule-based system, which follows different stages: (I) predominant wave direction; (II) specific characteristics of the devices to be installed; (III) mesh creation.

Each area was filled with the corresponding converters for the different desalination plants to meet the annual energy demand. The implementation criteria adopted were: (i) to minimize the number of rows; and (ii) within each row generated, to maximize the number of devices housed. However, the geometric capacity of the area may be insufficient to accommodate the total number of units required.

A visual example of the procedure used is shown in Figure 5, where the different wave farm configurations corresponding to the Las Palmas III desalination plant are detailed. At this location, the 1.5 km exclusion zone from the coastline coincides with the boundary imposed by environmental restrictions, so both design Scenarios (2 and 3) share the same operational polygon.

2.7. Step 7: Wave Farms vs. PV Farms Surface Covered

In isolated systems and/or those with a limited surface area, such as the Canary Islands, one of the key parameters for comparing technologies is the amount of surface area occupied by each farm. PV technology was selected for this comparison due to its predominant use in desalination complexes.

The area occupied by a photovoltaic farm can be estimated using Equation (1). First, the main characteristics of the photovoltaic panel must be determined, such as panel efficiency. Then, the conditions of the park's location must be considered, such as electrical and other farm losses (PR), annual global inclined irradiance (GTI), and the ratio between the necessary panel area and the total area of the park (GCR).

$$A_{PV\_farm} = \frac{D_e \times C_{wave} \times \eta_P \times PR}{GTI \times GCR} \quad (1)$$

where

A_{PV_farm}: PV farm area (m^2).
D_e: Annual electrical demand from desalination plant (kWh/year).
C_{wave}: Coverage of electricity demand by the wave farm.
η_P: PV panel efficiency.
PR: Performance Ratio.
GTI: Annual Global Tilted Irradiance (kWh/m^2 year).
GCR: Ground Cover Ratio.

This enables a comparison to be made between the areas occupied by wave and PV farms, allowing a decision to be made in favour of one alternative based on land use criteria.

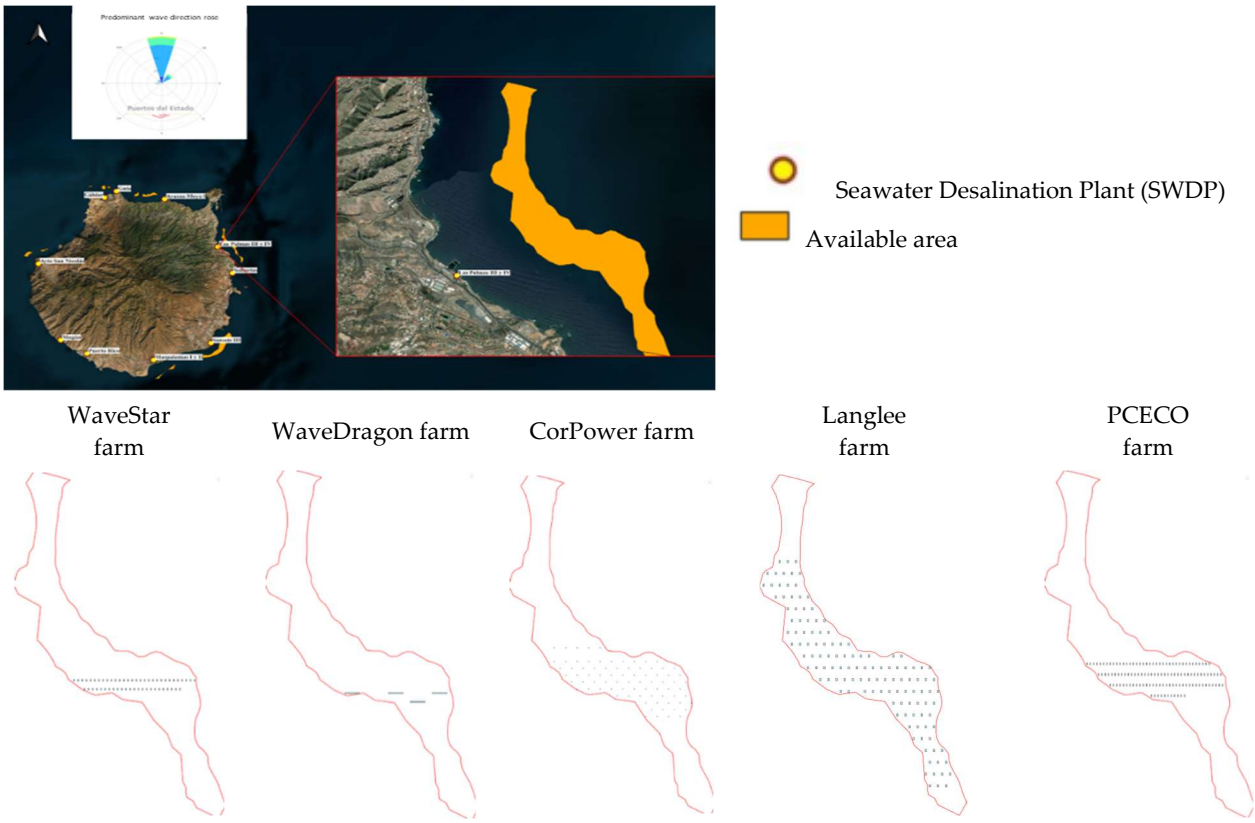

Figure 5. Configurations of the different wave energy farms for the Las Palmas III desalination plant, Gran Canaria, Spain.

3. Results and Discussion

This section presents and discusses the results derived from the three scenarios analyzed in this study. Each scenario was modelled using identical resource and energy demand data. The first scenario considers the best device in each area based on the resource, while the other two scenarios are wave energy farm configurations that prioritize demand coverage and power density, allowing for a direct comparison of the impact of these factors on the energy viability and efficiency of the farm.

3.1. Wave Resource and Potential Area Assessment

The Canary Islands archipelago, located in the North Atlantic swell corridor, has one of the highest wave energy potentials in Europe, with an average annual energy density of 18–25 kW/m on its north-western coasts [95]. In addition, its unique volcanic geomorphology features steep underwater slopes that descend from the coastline to abyssal depths in less than 1 km. This relief generates a critical oceanographic phenomenon where waves experience an exponential increase in height and slope as they approach the coast due to interaction with the seabed.

Figure 6 shows, by island, maps of potential areas within a 5 km radius of desalination complexes and how these areas are affected by the 1.5 km distance restriction from the coastline. A maximum bathymetry of 50 m is used, as this is a limiting factor in WEC operation.

Figure 6. Map of potential areas with a 1.5 km safety restriction.

These potential areas were subjected to the application of environmental restrictions and marine-use compatibility. Figure 7 shows the results of this application using the island of Gran Canaria as a reference.

Table 5 shows the potential available area for each island and its change after application of the safety distance and environmental restrictions.

Table 5. Evolution of available area.

Island	Potential Area. Scenario 1 (km^2)	Available Area with 1.5 km Safety Restriction. Scenario 2 (km^2)	Available Area After Applying Environmental Restrictions. Scenario 3 (km^2)
Lanzarote	10.32	1.02	0.90
Fuerteventura	26.80	18.89	0.35
Gran Canaria	98.64	67.32	28.98
Tenerife	19.76	1.41	0.10
El Hierro	2.63	0.00	0.00

The values obtained demonstrate how the necessary implementation of restrictions affects the potential area. On the islands of Lanzarote, Tenerife, and El Hierro, it can be seen that the most significant reduction in usable area occurs when applying the restriction of a minimum distance of 1.5 km from the coast. This safety criterion particularly affects the westernmost islands of El Hierro and Tenerife, where the relief and rapid bathymetric slope cause the seabed to deepen in a very short horizontal distance. As a result, when this limitation is applied, the available area is reduced by more than 90%, reaching 100% in the case of El Hierro.

With regard to the difference in area between Scenarios 2 and 3, the impact of environmental restrictions on the final available area is most evident in the case of Fuerteventura, where the available area is reduced by more than 98%.

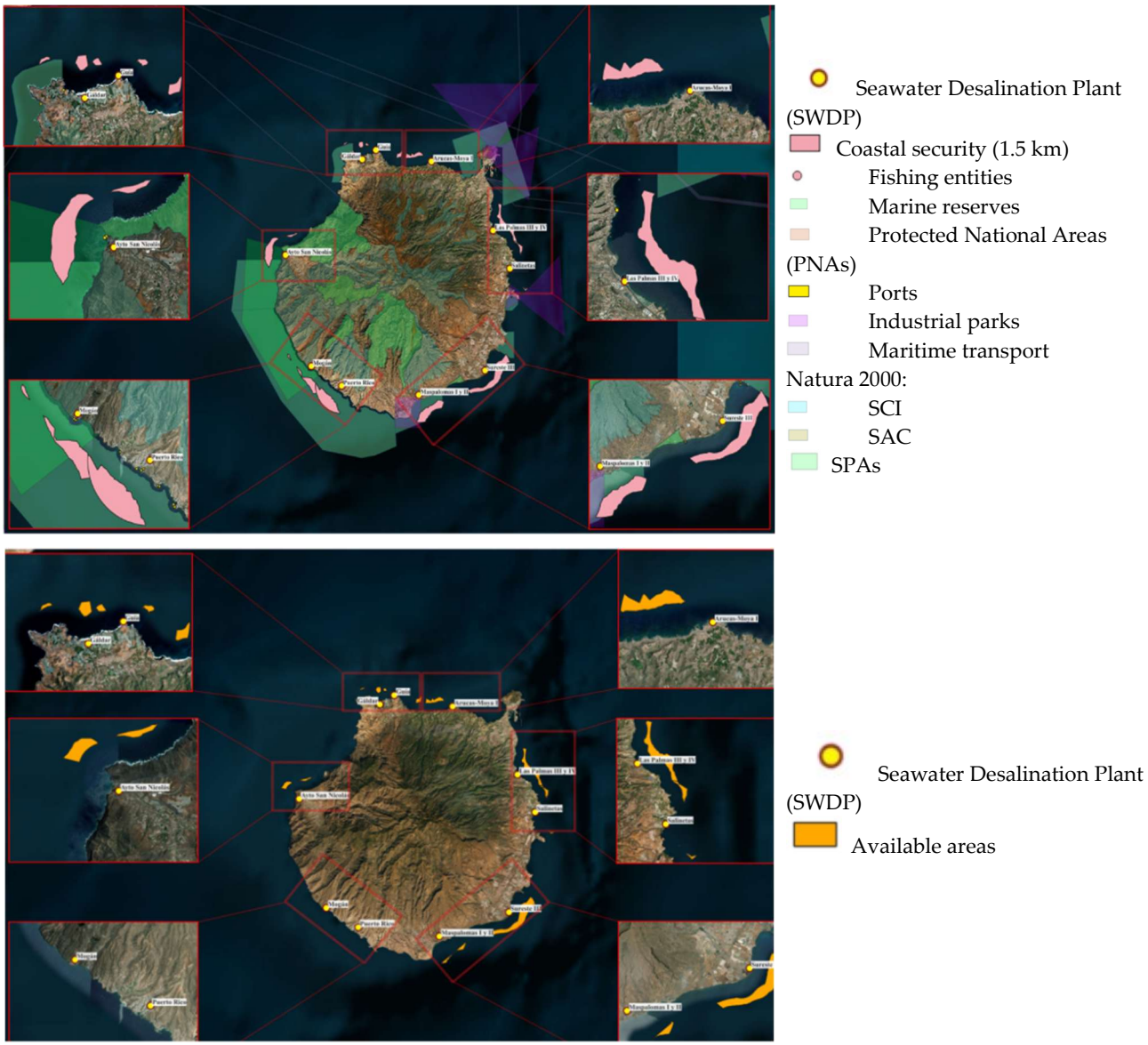

Figure 7. Identification of the applied restrictions (**top**) and the resulting available areas for wave energy development (**bottom**) on the island of Gran Canaria.

3.2. Single Device Design: Scenario 1

The first scenario identifies which of the analyzed devices best matches the wave resource in individual format for each location. The device with the highest EH and CF combination is considered optimal in this context.

The analysis of the island of Lanzarote reveals two clearly differentiated wave regimes. At the Díaz Rijo SWDP, located on the east coast, the resource offers low energy levels that limit the CF to a maximum of 15%. The most suitable converter is the WaveStar model, with an EH value of 1289. In contrast, at the Janubio SWDP, located on the west coast, the resource is significantly higher. The Wave Dragon EH value is 3457 with a CF of 39%, making it the most suitable option for that location.

In Fuerteventura, wave energy resources are generally low, as the desalination plants are located in the eastern part of the island. However, Corralejo plant stands out with CF values of up to 35% and the Wave Dragon converter with an EH value of 3063. It should be noted that the best-case scenario in Fuerteventura is an EH value of 1528 and a CF of 17%.

In the northern half of Gran Canaria, the waves are regular and powerful enough for WaveStar to operate with EH values between 2583 and 3290, and CFs ranging from 29% to 38%. Wave Dragon performs in a similar, slightly lower, EH range of between 2415 and 3185. In this case, the exposed Atlantic front maintains a wave spectrum that favors these two technologies, allowing an energy coverage ratio of up to 17% with a single WaveStar unit in Guía. The south and southeast arc (Mogán, Puerto Rico, Maspalomas, Sureste and Salinetas) has a significantly lower resource. WaveStar falls to EH values between 676 and 1580, with CFs of 8–18%, and Wave Dragon to EH values of 662-1035 and CFs of 8–12%, highlighting the lower wave energy resource in this area and emphasizing the impact of the island's shadow. The EH values and energy capacity ratios for the CorPower, Langlee and PCECO technologies remain below 1500 and 23%, respectively, at all these southern sites, reinforcing the conclusion that wave energy productivity in the south of the island is limited for single-device configurations. With regard to the center of the island, where the plant with the highest demand is located, the same pattern occurs as observed in the north. WaveStar records an EH value of 3050 and a CF of 35%, confirming the quality of the resource in the area. However, with these characteristics in a single device configuration, it barely covers 2% of the desalination plant's annual consumption.

On the western side of Tenerife Island, the waves allow Wave Dragon to operate for 1176 EH per year with a CF of 13% and cover almost 63% of the demand of a medium-sized desalination plant. For its part, WaveStar has an EH value of 1031 and a CF of 12%. Moving northeast, the regularity of the resource improves: in Santa Cruz, WaveStar reaches an EH value of 2514 per year and a CF of 29%, and Wave Dragon an EH of 1930 and a CF of 22%. The southern sector shows a clear decline in potential. In Granadilla, the only site with an EH value above 2600 in the area, the WaveStar EH value is 2673 and its CF is 31%, almost twice as high as Wave Dragon, with an EH value of 1365 and CF of 16%. Further southwest, Arona and La Caleta fall to EH values of 550 for Wave Dragon and 463 for WaveStar, with CFs of 6% and 5%, respectively. At these sites, CorPower, Langlee and PCECO technologies also remain below EH and 14% capacity, confirming that wave energy performance in the southern area is insufficient for the installation of a single device.

El Hierro island has the most favorable wave conditions in the study due to its geographical location, as it is the island most exposed to waves from the North Atlantic. In Los Cangrejos and El Golfo, conditions allow WaveStar to exceed EH values of 3700 and 3500, respectively, with CFs of 43% and 41%. The corresponding Wave Dragon values are only slightly lower at both locations, confirming a very constant resource that maximizes the use of both terminators and multiple float devices. The CorPower, Langlee and PCECO EH values range between 2260 and 610 for the same sites, showing a clear hierarchy with WaveStar and Wave Dragon dominating unit production. La Restinga, located on the southern slope, shows a less energetic resource, but still notable in comparison with other islands. The WaveStar EH and CF values of 2766 and 32% comfortably exceed the corresponding values for Wave Dragon of 2066 and 24%. The remaining technologies fall below EH and CF values of 1400 and 15%, respectively. These values make WaveStar the most efficient option for single-device operations throughout El Hierro, although Wave Dragon is also competitive in the north and east due to the high absolute power it can feed into the desalination system.

Figure 8 summarizes all the results, comparing WaveDragon, WaveStar, and CorPower performances in terms of EH and the energy coverage ratio achieved by each device. The bars represent the two technologies with the highest EH values at each site. WaveDragon and WaveStar dominate in most locations, while CorPower outperforms the others only in two areas of Tenerife Island (Arona and La Caleta), where its compact design adapts well to local wave conditions and spatial constraints. Figure lines show the energy coverage

percentage, represented by two curves: one corresponding to the best-performing device and the other to the second best in each study area. In many locations, the technologies exceed 2400 EHs, indicating an effective utilization of the marine resource.

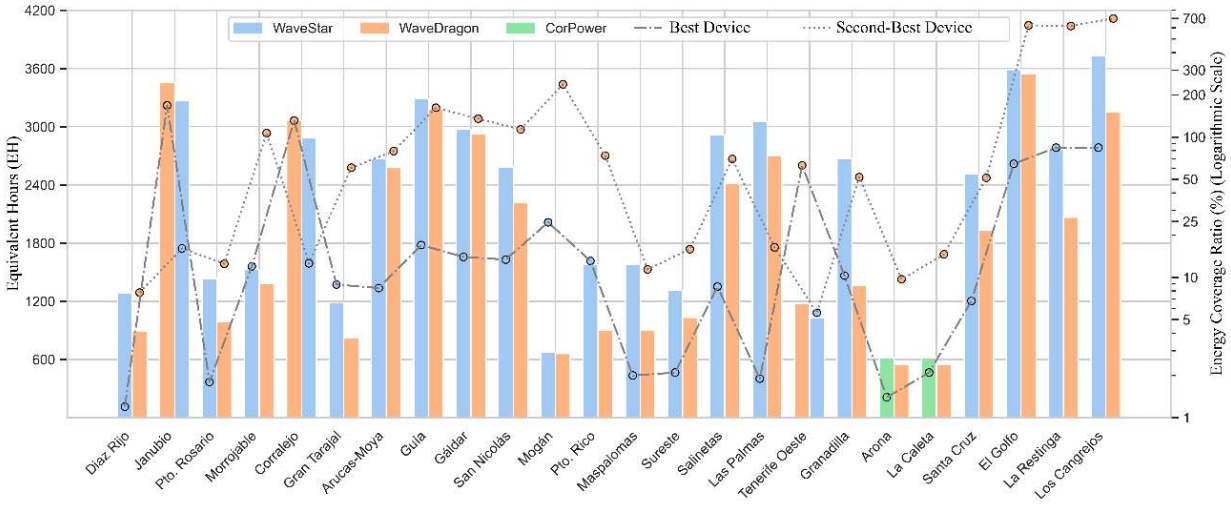

Figure 8. Comparison of EHs and energy coverage ratio by location in Scenario 1.

WaveDragon consistently achieves the highest energy coverage ratios. This is due to its devices having a much higher rated power than those of WaveStar, allowing it to meet a larger share of demand with fewer units installed.

3.3. Scenario 2: Wave Farm Configuration Results

This second scenario introduces the configuration of wave farms within areas restricted solely by the 1.5 km coastal exclusion zone (see Figure 7). Consequently, the percentage of coverage to meet the energy demand of the desalination plant is adopted as the main criterion for comparison. If similar coverage values are achieved, the installed power density, understood as the ratio between the total installed power of the farm and the area actually occupied, is assessed. In addition, the number of devices that need to be installed are taken into consideration when choosing the optimal configuration in each circumstance, prioritizing the lowest number.

In this way, Scenario 2 explicitly focuses on the spatial and energetic efficiency of each technology, evaluating how much useful power can be deployed per unit of occupied marine area and per installed device when only the coastal setback constraint is active.

The island of Lanzarote has only one potential area available after the applied restrictions. This is the coastal area adjacent to the Díaz Rijo desalination plant (see Figure 7). The configuration with 67 WaveStar devices and 40.2 MW installed is the optimal solution, offering the maximum energy coverage among the alternatives, meeting 77% of the annual demand within the available area, with a density of 39.5 MW/km. The CorPower, PCECO and Langlee alternatives are well below this, with coverage of 15%, 28% and 11%, respectively, while a single Wave Dragon contributes only 8%, given that the large minimum distances required between Wave Dragon devices to avoid interference restrict installation to a single unit and therefore drastically limit its energy contribution in the available area.

The Lanzarote results therefore show that, in narrow coastal polygons, technologies with smaller footprints and shorter spacing requirements, such as WaveStar, use the available strip much more efficiently than large-scale alternatives, which cannot exploit the full polygon due to their minimum separation distances.

For the island of Fuerteventura, the Puerto del Rosario desalination plant (central area of the island) does not achieve 100% coverage with any proposal. The wave farm

with 28 WaveStar devices covers 51% of demand and clearly outperforms the other configurations, which cover less than 20% of demand. This makes WaveStar the only option that meets the coverage criteria in this location, providing an installed power density of 35 MW/km^2. In contrast, the Corralejo desalination plant (north of the island) presents the opposite scenario. A single Wave Dragon device covers 131% because the resource conditions in Corralejo greatly favor a Wave Dragon farm, a ratio that exceeds that achieved by WaveStar, CorPower, Langlee and PCECO. Only one device is needed, as the plant's energy demand is not very intense. Finally, at the Gran Tarajal desalination plant (south of the island), several technologies meet or exceed demand, but the farm with two Wave Dragons is once again the dominant technology with 121% coverage. Its density, identical to that recorded in Corralejo at 568 MW/km^2, is also the highest of the group.

At the northern half of Gran Canaria locations (Arucas-Moya, Guía, Gáldar, San Nicolás and Las Palmas), all configurations achieve at least 100% coverage, so the selection criterion is decided by installed power density. In Arucas-Moya, the two Wave Dragon devices concentrate 11.8 MW in 0.021 km^2 and reach 567 MW/km^2, the maximum density of the group, making it the optimal option. In Guía, Gadar and San Nicolás, only one Wave Dragon device needs to be installed to cover the energy demand. Therefore, Wave Dragon is chosen as the optimal solution for coverage and to minimize the installation of devices. In Las Palmas, WaveStar is the optimal technology to install in a farm layout to fully cover demand, registering 88.8 MW/km^2, while Wave Dragon covers 57% of demand and the other technologies do not match its density. Maspalomas and Sureste (the other side of the island) Wave Dragon farms do not reach 100% coverage due to the island's orographic shadow effect. The wave resource in these areas has attenuated heights and periods that fall outside the optimal operating range of Wave Dragon. Among the alternatives that meet the requirements, WaveStar offers the highest installed power density, 66.5 MW/km^2 in Maspalomas and 75.4 MW/km^2 in Sureste, with a moderate number of units and footprint, making it the optimal choice for these two locations

Thus, in the northern sites, the combination of regular Atlantic swell and compact polygons allows Wave Dragon to maximise installed power per square kilometre with very few units, whereas in the shadowed southern and southeastern sites, the reduced wave climate makes medium-scale devices such as WaveStar more efficient in converting the available resource into usable power within the same marine footprint.

Finally, on the island of Tenerife, the CorPower device obtained the best EH and CF values on the south-west coast, at the Arona and La Caleta desalination plants. WaveStar and CorPower achieved the coverage target at La Caleta in particular, with CorPower the best alternative due to the need to use half the number of devices. In the other potential area, the southeast with the Granadilla desalination plant, no technology covers more than 32% of the demand. CorPower provides the highest value of 37.5 MW/km^2, outperforming WaveStar, PCECO and Langlee.

Figure 9 summarizes the performance of different WECs in Scenario 2. Wave Dragon stands out for its ability to install a large amount of power with relatively few devices. This is due to its high nominal power per unit, which results in a greater installed power density—clearly represented by the blue bars. The locations without bars mean that a single device is sufficient to meet the energy demand or occupy the available area. In these cases, displaying an additional density value would not be meaningful.

From the perspective of spatial efficiency, the sites where Wave Dragon displays the highest bars correspond precisely to those polygons where the technology achieves the greatest concentration of installed capacity per unit area, which is particularly relevant for islands with very limited suitable marine space.

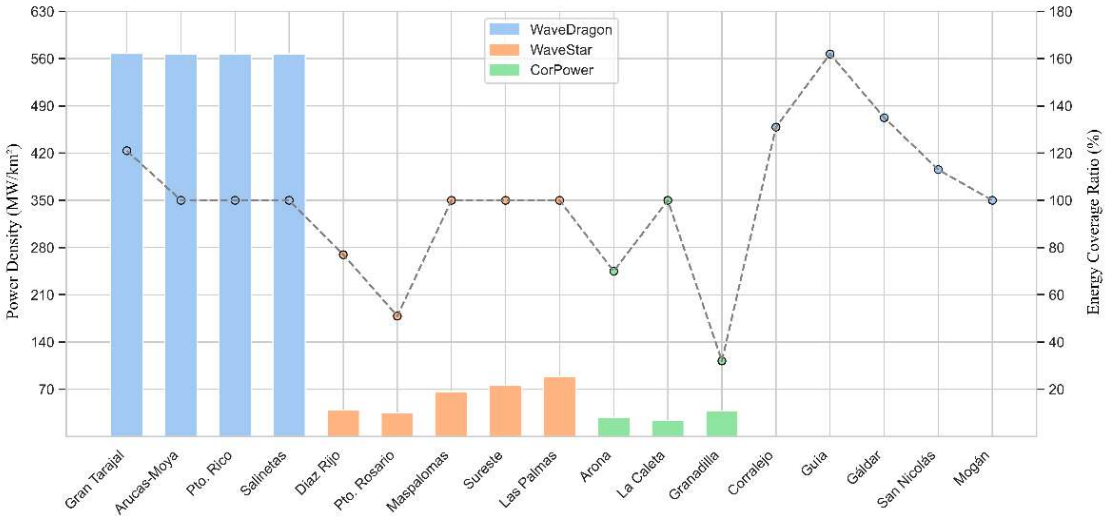

Figure 9. Power density and energy coverage ratio by location in Scenario 2.

The line chart shows the percentage of energy coverage at each site. Most values exceed 100%, indicating that energy production surpasses desalination demand. This confirms that wave energy can meet energy needs while using only a small portion of the marine space. This behavior follows the trend observed in the previous scenario. Wave Dragon and WaveStar continue to stand out as high-performance options in terms of installed power and coverage. CorPower, on the other hand, performs more efficiently in certain areas of Tenerife, where its smaller size and flexible configuration are better suited to the local conditions.

From an efficiency point of view, coverage values above 100% indicate that the same arrays could be downsized or their surplus production redirected to other loads while still meeting desalination demand, providing design flexibility without increasing the occupied marine area.

Therefore, Scenario 2 shows that the most suitable WECs are those that simultaneously optimize energy coverage, installed power density and number of units, maximizing the amount of useful energy that can be extracted per unit of occupied sea surface under a single, clearly defined spatial constraint.

Overall, the results confirm that the analyzed technologies can effectively adapt to different spatial and energy contexts while making efficient use of the marine environment.

3.4. Scenario 3: Wave Farm Configuration with Environmental Restrictions

In this third scenario, wave energy farms are sized applying not only the 1.5 km coastal safety zone but also all the environmental restrictions identified. The incorporation of these restrictions reduces the usable areas and substantially modifies the available surface at most sites. However, it can serve as a roadmap for the deployment of this type of renewable energy, indicating areas that are more suitable for initial implementation.

Figure 10 shows the potential areas for wave farm development after applying all environmental and infrastructure restrictions.

The same criteria of energy coverage, installed power density and minimum number of devices installed will be maintained for the selection of the optimal device configuration. Table 6 summarizes the selected technology, the area occupied by its implementation, and the coverage of energy demand.

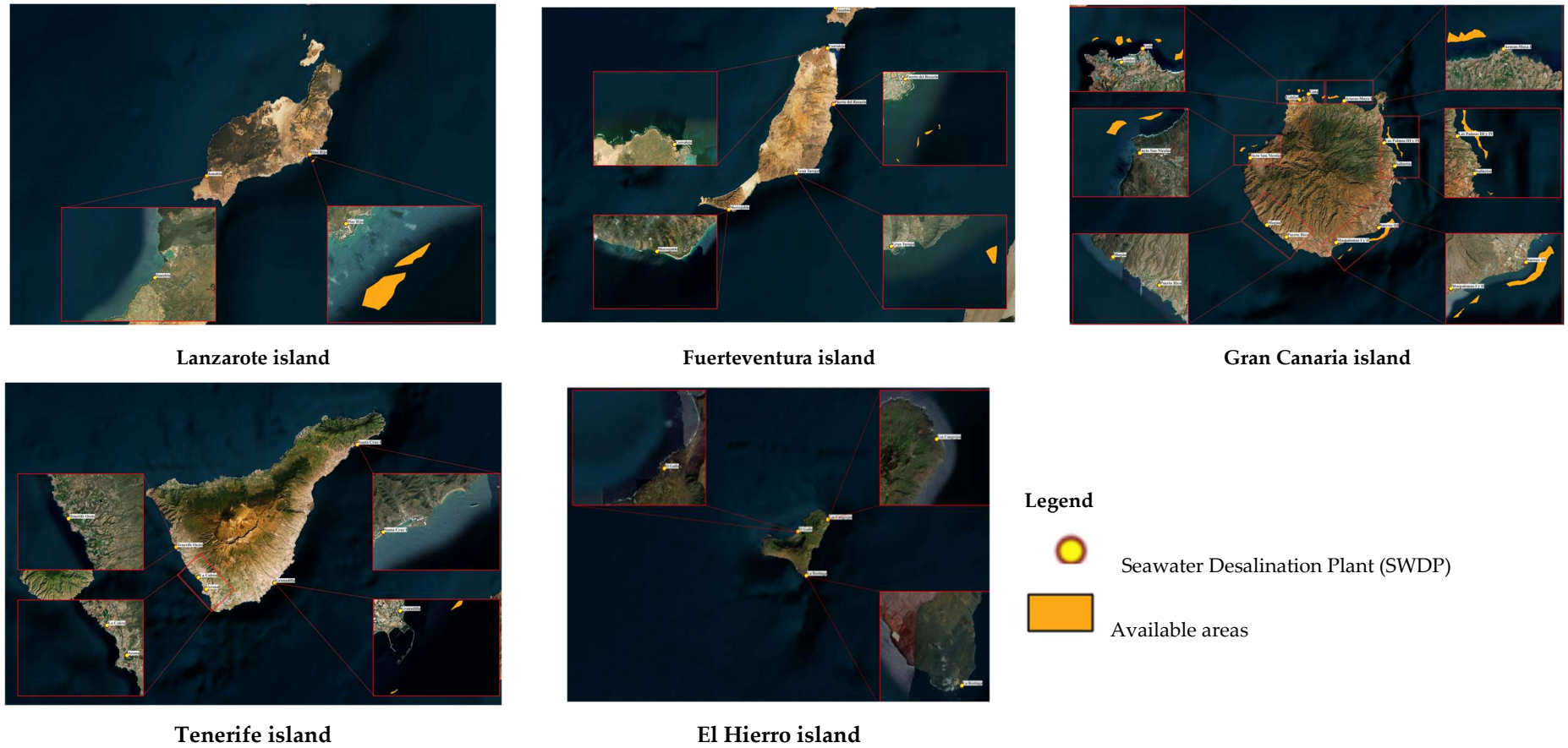

Figure 10. Map of potential areas after environmental and infrastructures constraints (Scenario 3).

Table 6. Summary of technologies selected for wave energy farms in Scenario 3.

SWDP	WEC	SWDP Energy Demand (GWh/Year)	Energy Coverage (%)	Area Available After Restrictions (km^2)	Farm Area (km^2)
Lanzarote Island					
Diaz Rijo	WaveStar	66.9	67	0.900	0.900
Fuerteventura Island					
Pto. Del Rosario	WaveStar	46.63	11	0.060	0.040
Gran Tarajal	WaveStar	8.03	100	0.290	0.064
Gran Canaria Island					
Arucas-Moya	Wave Dragon	19.16	100	2.190	0.021
Gáldar	Wave Dragon	11.61	270	2.270	0.021
Guía I y II	Wave Dragon	12.78	324	1.380	0.021
Ayto. San Nicolás	Wave Dragon	11.54	100	6.170	0.021
Las Palmas III y IV	WaveStar	97.24	100	6.040	0.365
Maspalomas I y II	WaveStar	46.51	100	1.810	0.750
Sureste III	WaveStar	38.33	100	11.730	0.390
Salinetas	Wave Dragon	20.44	100	1.400	0.021
Tenerife Island					
UTE Granadilla	CorPower	15.53	32	0.100	0.100

The results show that, after applying all spatial and environmental restrictions, only two types of wave energy devices are capable of maintaining the best installed power density to meet the energy demand of production centers with available space. Under the same depth and orientation constraints, Wave Dragon and WaveStar achieve the highest areal energy productivity ($GWh \cdot km^{-2} \cdot year^{-1}$), which explains why they remain as the only competitive options once all restrictions are applied. In practice, both technologies allow for the optimization of the available area, either by distributing a WaveStar network or by installing a small number of Wave Dragon terminators, as they guarantee the energy self-sufficiency of the desalination plants in most of the cases analyzed.

Figure 11 combines bars and a line to display two variables for Scenario 3. The bars represent power density in MW per square kilometer for the Wave Dragon, WaveStar, and CorPower technologies. The line shows the percentage of energy coverage at each site.

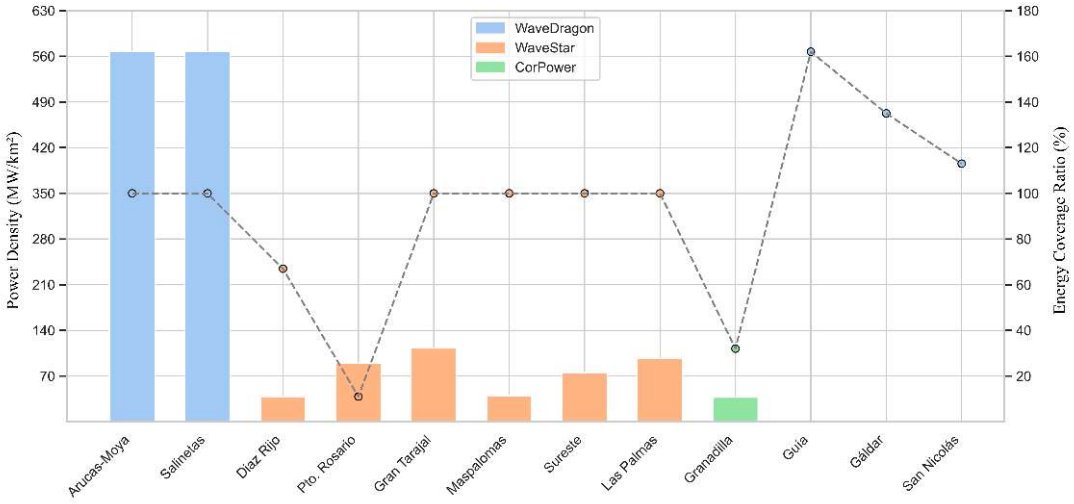

Figure 11. Power density and energy coverage ratio by location in Scenario 3.

In this scenario, the study areas are smaller and, in some cases, differ in shape. This affects the potential for device installation and resource utilization. Nevertheless, most sites achieve coverage close to or equal to 100%, demonstrating that wave energy is well adapted to spatial constraints. The results indicate that Wave Dragon achieves a high-power density, mainly due to its larger size, which allows it to generate more energy within a smaller footprint. WaveStar and CorPower show lower power densities but still maintain acceptable coverage levels.

The geometry of the available polygons plays a key role in this behaviour: compact polygons with sufficient width along the predominant wave direction allow regular array layouts with limited hydrodynamic interference between rows, enhancing the effective conversion efficiency per unit area. Conversely, narrow or highly fragmented polygons constrain the length of device rows and increase edge effects, reducing the achievable installed power density even where the local wave climate is energetic. The sites that reach coverage values close to 100% are precisely those where polygon shape and size enable an efficient packing of devices within the restricted marine space.

Overall, the graph illustrates that even with a reduced available area, wave energy retains a strong performance, making it a suitable option for islands or other regions with limited space.

In order to properly consider the potential for implementing wave energy, Figure 12 compares the space required by a wave energy farm and a PV farm to generate the same amount of energy at different study locations. The green area represents the surface occupied by the wave energy farm, while the orange area corresponds to the PV farm. The PV technology was selected due to its predominant use in desalination complexes.

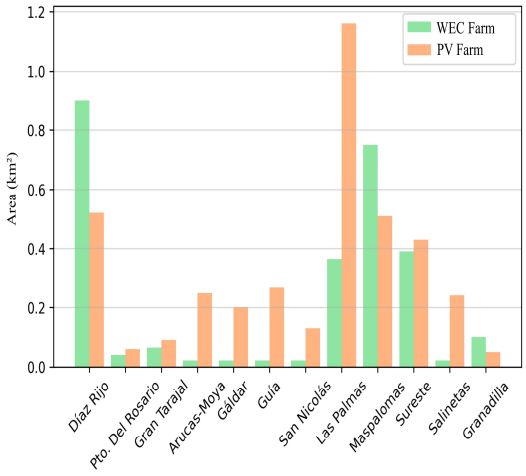

Figure 12. Comparative analysis of required area. Wave technology vs. solar photovoltaic technology.

The following factors were considered when calculating the PV surface area: a photovoltaic panel efficiency of 23.3% [96], a performance ratio (*PR*) of approximately 0.85 [97] and a ground coverage ratio (*GCR*) of 19.5% [97]. Likewise, the annual global tilted irradiance (*GTI*) was obtained from the PVGIS tool for each studied location.

In almost all cases, the wave energy farm requires less space. This is because ocean waves concentrate more energy per unit area than solar radiation. As a result, a more compact installation can achieve the same power output. The marine location of this technology also offers the advantage of not occupying agricultural land or areas that could be used for urban or landscape purposes. By avoiding competition for land use, it prevents territorial conflicts and minimizes any visual impact.

Overall, the graph demonstrates how wave energy can make more efficient use of space and complement other renewable sources in islands and coastal regions.

In Arucas-Moya, Galdar, Guía, San Nicolás and Salinetas, Wave Dragon is the optimal wave farm configuration. Compared to wave technology, the PV installation would require between eight and twelve times more surface area to cover the same energy demand of these desalination plants. The result highlights the advantage of wave technology, which also occupies a surface area that has a considerably lower impact on society in general.

At the Gran Tarajal and Sureste III sites, WaveStar is the optimal technology to implement. The global horizontal radiation exceeds 2300 kWh/m^2 per year, but even with this solar resource, the PV plant at these two locations needs 10% and 41% more land, respectively, to provide the same energy coverage.

The Las Palmas III-IV location has a very high energy demand (97 GWh/year), but 54 WaveStar units could be installed to cover the annual energy demand of the desalination plant. To supply the same 100% through a PV plant, 1.16 km^2 would be required, which corresponds to a surface area twice as large. With regard to the Díaz Rijo, Maspalomas and Granadilla plants, a wave energy farm with the same configuration of devices, even covering 100% of the necessary installed power, occupies 42%, 32% and 45% less space, respectively, than its PV counterparts. This combines low installed power density in these locations for wave energy farm configurations with, in contrast, very high average annual solar irradiance.

Only where low installed power density in wave farms is combined with very high average annual solar irradiance can PV technology improve the situation. This is the case at the Díaz Rijo, Maspalomas and Granadilla plants, where PV technology covers 42%, 32% and 45% less surface area, respectively, than wave energy to meet the entire energy demand.

Nevertheless, analyzing the variability of wave energy with the values provided by solar-PV, a future line of research could be the combination of both technologies in each of the areas studied. Figure 13 shows how wave energy varies throughout the seasons. As can be seen, the eastern and south-eastern areas of the islands do not experience significant changes, unlike the northern and north-western areas. In the latter locations, variability (mainly between summer and winter) is more pronounced, and the use of energy storage systems or hybridization with other renewable technologies may be necessary to ensure grid stability and security of supply in desalination plants that show constant energy consumption throughout the year. This would require a more detailed analysis of each specific plant, as well as other possible renewable resources available in the area.

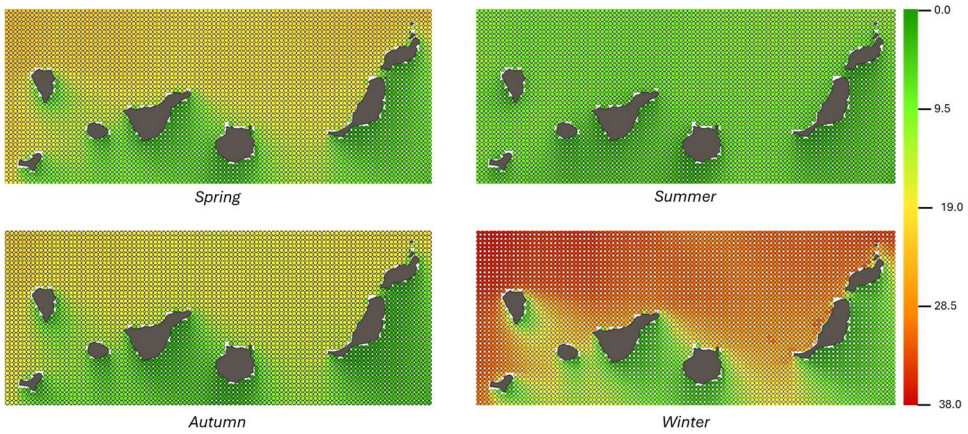

Figure 13. Wave energy potential of the Canary Islands in different seasons of the year (kW/m).

4. Conclusions

This research determines whether wave converters can be effectively integrated into seawater desalination treatment plants to reduce fossil fuel dependency in a region of water scarcity which is strongly dependent on this kind of water resource.

The study compared five technologies—WaveStar, WaveDragon, CorPower, Langlee, and PCECO—subjecting them to three scenarios with increasing degrees of restriction. The Canary Archipelago was chosen as case study. The first scenario evaluated the unit performance of each device in relation to the available wave resource near the desalination complexes. In this context, WaveStar proved to be the most operationally robust option, recording the highest equivalent hours (3290 h-Gran Canaria island) and the highest capacity factor (41%-El Hierro island) in virtually all locations, making it the benchmark for use when available space is limited or when only a complementary energy supply is required.

The second scenario shifted the analysis to a wave farm layout within a strip located one and a half kilometres from the coast and at depths of between thirty and fifty meters (WEC operating bathymetries), with the aim of maximising the energy coverage of the desalination facilities. It is confirmed that 88% of the desalination plants in the scenario could supply their annual energy consumption with this renewable technology. The results showed that Wave Dragon and WaveStar configurations achieve the highest production levels and best installed power densities, each offering different advantages: the first device concentrates high power in a few units (with the best value of 567 MW/km^2 in Gran Canaria Island), while the second offers greater modularity and better resistance to adverse conditions.

The third scenario incorporated regulated environmental restrictions and the presence of protected areas (which results in a 90% reduction in usable marine area on some islands, leading to the exclusion of the island of El Hierro from the study). Under these conditions, Wave Dragon and WaveStar once again led the way, confirming that both technologies remain competitive even when the usable surface area is significantly reduced. The proposed configuration for each island is thus supported by a balance between desalination plant energy demand coverage achieved and marine surface area occupied, which enables the energy consumption of 75% of the plants in the scenario to be met.

To confirm the effective performance of wave energy farms, a direct comparison was made with photovoltaic plants sized to match the same energy demand ratio. The comparison showed that only in three of the cases analyzed did the PV plant, in its ideal configuration on horizontal ground at an optimum angle, achieve a lower footprint. In the rest, the wave converter farm demonstrated a more favorable spatial footprint thanks to its high-power density.

Author Contributions: Conceptualization, B.D.R.-G., A.J.Y.-R., and P.Y.R.; methodology, B.D.R.-G. and A.J.Y.-R.; software, A.J.Y.-R. and P.Y.R.; validation, B.D.R.-G. and P.Y.R.; formal analysis, B.D.R.-G.; investigation, B.D.R.-G., A.J.Y.-R., and P.Y.R.; resources, B.D.R.-G., A.J.Y.-R., P.Y.R., and J.S.-R.; data curation, A.J.Y.-R.; writing—original draft preparation, B.D.R.-G.; writing—review and editing, B.D.R.-G. and A.J.Y.-R.; visualization, B.D.R.-G., P.Y.R. and J.S.-R.; supervision, B.D.R.-G.; project administration, J.S.-R. and B.D.R.-G.; funding acquisition, J.S.-R. and B.D.R.-G. All authors have read and agreed to the published version of the manuscript.

Funding: This research was cofinanced with ERDF funds, through the INTERREG MAC 2021–2027 programme and the IDIWATER project (1/MAC/1/1.1/0022), integrated in the DESAL + Living Lab Platform (desalinationlab.com), and the Specific Research Fund: Route to Energy Transition in the Canary Islands (F2024/03) from the University of Las Palmas de Gran Canaria.

Data Availability Statement: The datasets utilized in this study are national accessible public datasets, freely available at: https://portus.puertos.es/# (accessed on 21 March 2024).

Conflicts of Interest: The authors declare no conflicts of interest.

Abbreviations

The following abbreviations are used in this manuscript:

RO	Reverse Osmosis
SD	Scatter diagram
RE	Renewable energy
PV	Solar photovoltaic
SWDP	Seawater Desalination Plant
SPA	Special Protection Area for birds
SAC	Special Areas of conservation
SCI	Sites of community Importance
PNA	Protected Natural Area
WEC	Wave Energy Converter
EH	Equivalent Hour
CF	Capacity Factor
AEP	Annual Energy Production
PR	Performance Ratio
GCR	Ground Coverage Ratio
GTI	Global Tilted Irradiance

References

1. Shahzad, M.W.; Burhan, M.; Ang, L.; Ng, K.C. Energy-water-environment nexus underpinning future desalination sustainability. *Desalination* **2017**, *413*, 52–64. [CrossRef]
2. Jones, E.; Qadir, M.; van Vliet, M.T.; Smakhtin, V.; Kang, S.-M. The state of desalination and brine production: A global outlook. *Sci. Total. Environ.* **2019**, *657*, 1343–1356. [CrossRef] [PubMed]
3. Li, Z.; Siddiqi, A.; Anadon, L.D.; Narayanamurti, V. Towards sustainability in water-energy nexus: Ocean energy for seawater desalination. *Renew. Sustain. Energy Rev.* **2018**, *82*, 3833–3847. [CrossRef]
4. Magni, M.; Jones, E.R.; Bierkens, M.F.; van Vliet, M.T. Global energy consumption of water treatment technologies. *Water Res.* **2025**, *277*, 123245. [CrossRef]
5. Qasim, M.; Badrelzaman, M.; Darwish, N.N.; Darwish, N.A.; Hilal, N. Reverse osmosis desalination: A state-of-the-art review. *Desalination* **2019**, *459*, 59–104. [CrossRef]
6. International Energy Agency. Electricity Generation Mix for Selected Regions, 2024. 2025. Available online: https://www.iea.org/data-and-statistics/charts/electricity-generation-mix-for-selected-regions-2024 (accessed on 13 October 2025).
7. Abdelkareem, M.A.; Assad, M.E.H.; Sayed, E.T.; Soudan, B. Recent progress in the use of renewable energy sources to power water desalination plants. *Desalination* **2018**, *435*, 97–113. [CrossRef]
8. Okampo, E.J.; Nwulu, N. Optimisation of renewable energy powered reverse osmosis desalination systems: A state-of-the-art review. *Renew. Sustain. Energy Rev.* **2021**, *140*, 110712. [CrossRef]
9. Scopus Research Database. Analysis of Topics/Areas of Research Published in the Desalination Sector Between 2020 and 2025. 2025. Available online: https://www.scopus.com/results/results.uri?st1=Desalination+sector&st2=&s=TITLE-ABS-KEY(Desalination+sector)&limit=10&origin=resultslist&sort=plf-f&src=s&sot=b&sdt=cl&sessionSearchId=bbad0762bf1e7341da85efde4ea20d07&cluster=scosubtype,%22ar%22,t,%22re%22,t (accessed on 12 November 2025).
10. Ayaz, M.; Namazi, M.; Din, M.A.U.; Ershath, M.M.; Mansour, A.; Aggoune, E.-H.M. Sustainable seawater desalination: Current status, environmental implications and future expectations. *Desalination* **2022**, *540*, 116022. [CrossRef]
11. Curto, D.; Franzitta, V.; Guercio, A. A Review of the Water Desalination Technologies. *Appl. Sci.* **2021**, *11*, 670. [CrossRef]
12. Sayed, E.T.; Olabi, A.; Elsaid, K.; Al Radi, M.; Alqadi, R.; Abdelkareem, M.A. Recent progress in renewable energy based-desalination in the Middle East and North Africa MENA region. *J. Adv. Res.* **2023**, *48*, 125–156. [CrossRef] [PubMed]
13. IRENA. Water Desalination Using Renewable Energy ENERGY TECHNOLOGY SYSTEMS ANALYSIS PROGRAMME. *Int. Renew. Energy Agency* **2012**, 1–28. Available online: https://www.irena.org/-/media/Files/IRENA/Agency/Publication/2012/IRENA-ETSAP-Tech-Brief-I12-Water-Desalination.pdf (accessed on 25 October 2025).
14. Azevedo, F.D.A.S.M. Renewable Energy Powered Desalination Systems: Technologies and Market Analysis. Master's Thesis, Department of Geographical, Geophysical and Energy Engineering, Faculty of Sciences, University of Lisbon, Lisbon, Portugal, 2014.
15. Walch, A.; Rüdisüli, M. Strategic PV expansion and its impact on regional electricity self-sufficiency: Case study of Switzerland. *Appl. Energy* **2023**, *346*, 121262. [CrossRef]

16. Ahmadi, E.; McLellan, B.; Mohammadi-Ivatloo, B.; Tezuka, T. The Role of Renewable Energy Resources in Sustainability of Water Desalination as a Potential Fresh-Water Source: An Updated Review. *Sustainability* **2020**, *12*, 5233. [CrossRef]
17. Qiblawey, Y.; Alassi, A.; Abideen, M.Z.U.; Bañales, S. Techno-economic assessment of increasing the renewable energy supply in the Canary Islands: The case of Tenerife and Gran Canaria. *Energy Policy* **2022**, *162*, 112791. [CrossRef]
18. Subramani, A.; Badruzzaman, M.; Oppenheimer, J.; Jacangelo, J.G. Energy minimization strategies and renewable energy utilization for desalination: A review. *Water Res.* **2011**, *45*, 1907–1920. [CrossRef]
19. Al-Karaghouli, A.; Kazmerski, L.L. Energy consumption and water production cost of conventional and renewable-energy-powered desalination processes. *Renew. Sustain. Energy Rev.* **2013**, *24*, 343–356. [CrossRef]
20. Keiner, D.; Salcedo-Puerto, O.; Immonen, E.; van Sark, W.G.; Nizam, Y.; Shadiya, F.; Duval, J.; Delahaye, T.; Gulagi, A.; Breyer, C. Powering an island energy system by offshore floating technologies towards 100% renewables: A case for the Maldives. *Appl. Energy* **2022**, *308*, 118360. [CrossRef]
21. Alshamaileh, D.; Quran, O.; Almajali, M.R. Study the effect of solar power on the efficiency of desalinating saline water: Case studies Al-Khafji and Gulf of Aqaba areas. *Adv. Mech. Eng.* **2024**, *16*. [CrossRef]
22. Schallenberg-Rodríguez, J.; Del Rio-Gamero, B.; Melian-Martel, N.; Alecio, T.L.; Herrera, J.G. Energy supply of a large size desalination plant using wave energy. Practical case: North of Gran Canaria. *Appl. Energy* **2020**, *278*, 115681. [CrossRef]
23. Lehmann, M.; Karimpour, F.; Goudey, C.A.; Jacobson, P.T.; Alam, M.-R. Ocean wave energy in the United States: Current status and future perspectives. *Renew. Sustain. Energy Rev.* **2016**, *74*, 1300–1313. [CrossRef]
24. Del Río-Gamero, B.; Alecio, T.L.; Schallenberg-Rodríguez, J. Performance indicators for coupling desalination plants with wave energy. *Desalination* **2022**, *525*, 115479. [CrossRef]
25. Franzitta, V.; Curto, D.; Milone, D.; Viola, A. The Desalination Process Driven by Wave Energy: A Challenge for the Future. *Energies* **2016**, *9*, 1032. [CrossRef]
26. de la Fuente, J.A. The Canary Islands experience: Current non-conventional water resources and future perspectives. In Proceedings of the Regional Conference Advancing Non-Conventional Water Resources Management in Mediterranean Islands and Coastal Areas: Local Solutions, Employment Opportunities and People Engagement, Birgu, Malta, 10–11 May 2018; p. 26. Available online: https://www.gwp.org/contentassets/aa500f6c8cb749d7ac324a4065395386/203.the-canary-islands-experience.pdf (accessed on 29 October 2025).
27. Leon, F.; Ramos-Martin, A.; Perez-Baez, S.O. Study of the Ecological Footprint and Carbon Footprint in a Reverse Osmosis Sea Water Desalination Plant. *Membranes* **2021**, *11*, 377. [CrossRef]
28. Cabrera, P.; Lund, H.; Carta, J.A. Smart renewable energy penetration strategies on islands: The case of Gran Canaria. *Energy* **2018**, *162*, 421–443. [CrossRef]
29. Benahmed, A.; Bessedik, M.; Abdelbaki, C.; Mokhdar, S.A.; Goosen, M.F.; Höllerman, B.; Zouhiri, A.; Badr, N. Investigating the long-term economic sustainability and water production costs of desalination plants: A case study from Chatt Hilal in Algeria. *Egypt. J. Aquat. Res.* **2025**, *51*, 31–38. [CrossRef]
30. Iglesias, G.; Carballo, R. Wave resource in El Hierro—An island towards energy self-sufficiency. *Renew. Energy* **2011**, *36*, 689–698. [CrossRef]
31. Iglesias, G.; Carballo, R. Wave power for La Isla Bonita. *Energy* **2010**, *35*, 5013–5021. [CrossRef]
32. Sierra, J.; González-Marco, D.; Sospedra, J.; Gironella, X.; Mösso, C.; Sánchez-Arcilla, A. Wave energy resource assessment in Lanzarote (Spain). *Renew. Energy* **2013**, *55*, 480–489. [CrossRef]
33. Veigas, M.; Iglesias, G. Wave and offshore wind potential for the island of Tenerife. *Energy Convers. Manag.* **2013**, *76*, 738–745. [CrossRef]
34. Choupin, O.; Del Río-Gamero, B.; Schallenberg-Rodríguez, J.; Yánez-Rosales, P. Integration of assessment-methods for wave renewable energy: Resource and installation feasibility. *Renew. Energy* **2022**, *185*, 455–482. [CrossRef]
35. Del Río-Gamero, B.; Choupin, O.; Melián-Martel, N.; Schallenberg-Rodriguez, J. Application of a revised integration of methods for wave energy converter and farm location pair mapping. *Energy Convers. Manag.* **2024**, *303*, 118170. [CrossRef]
36. Moharram, N.A.; Konsowa, A.H.; Shehata, A.I.; El-Maghlany, W.M. Sustainable seascapes: An in-depth analysis of multigeneration plants utilizing supercritical zero liquid discharge desalination and a combined cycle power plant. *Alex. Eng. J.* **2025**, *118*, 523–542. [CrossRef]
37. Leon, F.; Ramos, A.; Perez-Baez, S.O. Optimization of Energy Efficiency, Operation Costs, Carbon Footprint and Ecological Footprint with Reverse Osmosis Membranes in Seawater Desalination Plants. *Membranes* **2021**, *11*, 781. [CrossRef] [PubMed]
38. Canal Gestión Lanzarote. Desalación y Producción. Available online: https://www.canalgestionlanzarote.es/inicio/nuestro-ciclo-integral-del-agua/produccion-desalacion/ (accessed on 15 June 2025).
39. ELMASA. Mejora en la EDAM de Puerto Rico. 2020. Available online: https://elmasa.es/proyectos/proyecto-4/ (accessed on 13 July 2025).
40. Consejo Insular de aguas de Gran Canaria. Plan hidrológico de la isla de Gran Canaria. 2024. Available online: https://www.aguasgrancanaria.com/plan_hidro.php (accessed on 17 July 2025).

41. Consejo Insular de Aguas de El Hierro. Plan Hidrológico de la Isla de El Hierro. 2018. Available online: https://www.aguaselhierro.org/planificacion/plan-hidrologico/vigente/ (accessed on 22 July 2025).
42. Consejo Insular de Aguas de Tenerife. Plan Hidrológico de la Isla de Tenerife. 2018. Available online: https://aguastenerife.org/images/pdf/PHT1erCiclo/2_ciclo/ES124_PHD.pdf (accessed on 27 July 2025).
43. Consorcio de Abastecimiento de Aguas a Fuerteventura, "EDAM Gran Tarajal". 2021. Available online: https://caaf.es/el-caaf/dto-de-produccion/ (accessed on 11 August 2025).
44. Chirivella Guerra, J. Oral communication with the head of the water resources department of the Gran Canaria Island Water Council. 2025.
45. Cartográfica de Canarias—GRAFCAN. Ortofoto Territorial. 2022. Available online: https://visor.grafcan.es/ (accessed on 13 August 2025).
46. Veigas, M.; Carballo, R.; Iglesias, G. Wave and offshore wind energy on an island. *Energy Sustain. Dev.* **2014**, *22*, 57–65. [CrossRef]
47. Puertos del Estado. SIMAR Hindcast Database. Available online: https://www.puertos.es/servicios/oceanografia (accessed on 19 August 2025).
48. Losada, A.I.J.; Pascual, C.V.; Incera, F.J.M.; Solana, R.M.; Landeira, S.R.; Braña, P.C.; Sampedro, N.K.B.T. Evaluación Del Potencial de La Energía de Las Olas Estudio Técnico Plan Energias Renovables (PER) 2011–2020. 2021. Available online: https://www.idae.es/uploads/documentos/documentos_11227_e13_olas_b31fcafb.pdf (accessed on 20 August 2025).
49. Mérigaud, A.; Ringwood, J.V. Power production assessment for wave energy converters: Overcoming the perils of the power matrix. *Proc IMechE* **2018**, *232*, 50–70. [CrossRef]
50. Folley, M. *Numerical Modelling of Wave Energy Converters: State-of-the-Art Techniques for Single Devices and Arrays*; Academic Press: Cambridge, MA, USA, 2016.
51. Chang, G.; Jones, C.A.; Roberts, J.D.; Neary, V.S. A comprehensive evaluation of factors affecting the levelized cost of wave energy conversion projects. *Renew. Energy* **2018**, *127*, 344–354. [CrossRef]
52. Arean, N.; Carballo, R.; Iglesias, G. An integrated approach for the installation of a wave farm. *Energy* **2017**, *138*, 910–919. [CrossRef]
53. Choupin, O.; Têtu, A.; Del Río-Gamero, B.; Ferri, F.; Kofoed, J. Premises for an annual energy production and capacity factor improvement towards a few optimised wave energy converters configurations and resources pairs. *Appl. Energy* **2022**, *312*, 118716. [CrossRef]
54. Pascal, R.; Molina, A.T.; González, A. Going further than the scatter diagram: Tools for analysing the wave resource and classifying sites. In Proceedings of the 11th European Wave and Tidal Energy Conference, Nantes, France, 6–11 September 2015; pp. 5–12.
55. European Comission. EMODnet Portal. Available online: https://emodnet.ec.europa.eu/en/ (accessed on 27 November 2025).
56. Gobierno de España. Red Natura 2000: Cartografía. 2020. Available online: https://www.miteco.gob.es/es/biodiversidad/servicios/banco-datos-naturaleza/informacion-disponible/rednatura_2000_desc.html (accessed on 27 November 2025).
57. Gobierno de Canarias. Reservas Marinas de Canarias. 2019. Available online: https://www.gobiernodecanarias.org/pesca/temas/reservas_marinas/ (accessed on 22 September 2025).
58. Gobierno de Canarias. Espacios Naturales Protegidos (ENP). 2020. Available online: https://www.miteco.gob.es/es/cartografia-y-sig/ide/descargas/biodiversidad/enp.html (accessed on 27 November 2025).
59. Gobierno de España. La Red de Parques Nacionales. 2020. Available online: https://www.miteco.gob.es/es/parques-nacionales-oapn/red-parques-nacionales.html (accessed on 27 November 2025).
60. Gobierno de España. Reservas Marinas de España. 2020. Available online: https://www.mapa.gob.es/es/pesca/temas/proteccion-recursos-pesqueros/reservas-marinas-de-espana/default.aspx (accessed on 27 November 2025).
61. Gobierno de España. Ordenación del Espacio Marítimo. 2023. Available online: https://www.miteco.gob.es/es/cartografia-y-sig/ide/descargas/costas-medio-marino/poem.html (accessed on 27 November 2025).
62. Yanez-Rosales, P.; Del Río-Gamero, B.; Schallenberg-Rodríguez, J. Rationale for selecting the most suitable areas for offshore wind energy farms in isolated island systems. Case study: Canary Islands. *Energy* **2024**, *307*, 132589. [CrossRef]
63. Velázquez-Medina, S.; Santana-Sarmiento, F. Evaluation method of marine spaces for the planning and exploitation of offshore wind farms in isolated territories. A two-island case study. *Ocean Coast. Manag.* **2023**, *239*, 106603. [CrossRef]
64. Castro-Santos, L. Decision variables for floating offshore wind farms based on life-cycle cost: The case study of Galicia (North-West of Spain). *Ocean Eng.* **2016**, *127*, 114–123. [CrossRef]
65. Martinez, A.; Iglesias, G. Mapping of the levelised cost of energy from floating solar PV in coastal waters of the European Atlantic, North Sea and Baltic Sea. *Sol. Energy* **2024**, *279*, 112809. [CrossRef]
66. Jiang, H.; Yao, L.; Zhou, C. Assessment of offshore wind-solar energy potentials and spatial layout optimization in mainland China. *Ocean Eng.* **2023**, *287*, 115914. [CrossRef]
67. Fouz, D.; Carballo, R.; López, I.; Álvarez, B.; Iglesias, G. Floating solar photovoltaic energy for coastal areas: A siting methodology. *J. Clean. Prod.* **2025**, *528*, 146733. [CrossRef]

68. Wang, P.; Zhou, J.; Jin, X.; Shi, J.; Chan, N.W.; Tan, M.L.; Lin, X.; Ma, X.; Lin, X.; Zheng, K.; et al. The Impact of Offshore Photovoltaic Utilization on Resources and Environment Using Spatial Information Technology. *J. Mar. Sci. Eng.* **2024**, *12*, 837. [CrossRef]
69. Langlee Company. Langlee Wave Power. Available online: http://www.langleewp.com/e-brochure/ (accessed on 1 December 2025).
70. Sorensen, H.; Friis-Madsen, E.; Christensen, L.; Kofoed, J.P.; Frigaard, P.B.; Knapp, W. The results of two years testing in real sea of Wave Dragon. In Proceedings of the 6th European Wave and Tidal Energy Conference, Glasgow, UK, 29 August–2 September 2005.
71. Majidi, A.G.; Ramos, V.; Rosa-Santos, P.; das Neves, L.; Taveira-Pinto, F. Power production assessment of wave energy converters in mainland Portugal. *Renew. Energy* **2025**, *243*, 122540. [CrossRef]
72. CorPowerocean. CorPower Ocean's Wave Energy Converter Deployed in Portugal. Available online: https://corpowerocean.com/corpower-oceans-wave-energy-converter-deployed/ (accessed on 25 September 2025).
73. European Marine Energy Center. CorPower HiWave-3 at EMEC. Available online: https://tethys.pnnl.gov/project-sites/corpower-hiwave-3-emec (accessed on 25 September 2025).
74. Venugopal, V.; Tan, T. Hydrodynamic Assessment of the CorPower C4 Point Absorber Wave Energy Converter in Extreme Wave Conditions. In Proceedings of the ASME 2024 43rd International Conference on Ocean, Offshore and Arctic Engineering, Singapore, 9–14 June 2024; ISBN 978-0-7918-8785-1.
75. Al Shami, E.; Zhang, R.; Wang, X. Point Absorber Wave Energy Harvesters: A Review of Recent Developments. *Energies* **2019**, *12*, 47. [CrossRef]
76. Masoumi, M.; Estejab, B.; Henry, F. Implementation of machine learning techniques for the analysis of wave energy conversion systems: A comprehensive review. *J. Ocean Eng. Mar. Energy* **2024**, *10*, 641–670. [CrossRef]
77. Friss-Madsen, E. Personal communication with Managing Director of wave Dragon. 2021.
78. Holthuijsen, L.H. *Waves in Oceanic and Coastal Waters*; Cambridge University Press (CUP): Cambridge, UK, 2007.
79. García-Medina, G.; Özkan-Haller, H.T.; Ruggiero, P. Wave resource assessment in Oregon and southwest Washington, USA. *Renew. Energy* **2014**, *64*, 203–214. [CrossRef]
80. Reguero, B.G.; Losada, I.J.; Mendez, F.J. A global wave power resource and its seasonal, interannual and long-term variability. *Appl. Energy* **2015**, *148*, 366–380. [CrossRef]
81. *IEC TS 62600-101*; Marine Energy—Wave, Tidal and Other Water Current Converters—Part 101: Wave Energy Resource Assessment and Char-Acterization. International Electrotechnical Comission: Geneva, Switzerland, 2015; ISBN 9782832700365.
82. Fernandez, G.V.; Balitsky, P.; Stratigaki, V.; Troch, P. Coupling Methodology for Studying the Far Field Effects of Wave Energy Converter Arrays over a Varying Bathymetry. *Energies* **2018**, *11*, 2899. [CrossRef]
83. Stratigaki, V.; Troch, P.; Forehand, D. A fundamental coupling methodology for modeling near-field and far-field wave effects of floating structures and wave energy devices. *Renew. Energy* **2019**, *143*, 1608–1627. [CrossRef]
84. Troch, P.; Beels, C.; De Rouck, J.; De Backer, G. Wake effects behind a farm of wave energy converters for irregular long-crested and short-crested waves. In Proceedings of the International Conference on Coastal Engineering, Shanghai, China, 30 June–5 July 2010; Volume 30.
85. Beels, C.; Troch, P.; De Visch, K.; De Backer, G.; De Rouck, J.; Kofoed, J. Numerical simulation of wake effects in the lee of a farm of Wave Dragon wave energy converters. In Proceedings of the 8th European Wave and Tidal Conference: EWTEC 2009, Uppsala, Sweden, 7–11 September 2009.
86. Atan, R.; Finnegan, W.; Nash, S.; Goggins, J. The effect of arrays of wave energy converters on the nearshore wave climate. *Ocean Eng.* **2019**, *172*, 373–384. [CrossRef]
87. Babarit, A. On the park effect in arrays of oscillating wave energy converters. *Renew. Energy* **2013**, *58*, 68–78. [CrossRef]
88. Child, B.; Venugopal, V. Optimal configurations of wave energy device arrays. *Ocean Eng.* **2010**, *37*, 1402–1417. [CrossRef]
89. de Andrés, A.; Guanche, R.; Meneses, L.; Vidal, C.; Losada, I. Factors that influence array layout on wave energy farms. *Ocean Eng.* **2014**, *82*, 32–41. [CrossRef]
90. Bozzi, S.; Giassi, M.; Miquel, A.M.; Antonini, A.; Bizzozero, F.; Gruosso, G.; Archetti, R.; Passoni, G. Wave energy farm design in real wave climates: The Italian offshore. *Energy* **2017**, *122*, 378–389. [CrossRef]
91. Aristodemo, F.; Ferraro, D.A. Feasibility of WEC installations for domestic and public electrical supplies: A case study off the Calabrian coast. *Renew. Energy* **2018**, *121*, 261–285. [CrossRef]
92. Fernández Chozas, J. Una aproximación a la energía de las olas para la generación de electricidad. Final Degree Project. Department of Electrical Engineering. Higher Technical School of Industrial Engineering. Polytechnic University of Madrid. 2008. Available online: https://oa.upm.es/1203/1/PFC_JULIA_FERNANDEZ_CHOZAS.pdf (accessed on 28 August 2025).
93. Bastos, P.; Devoy-McAuliffe, F.; Arredondo-Galeana, A.; Chozas, J.F.; Lamont-Kane, P.; Vinagre, P.A. Life Cycle Assessment of a wave energy device—LiftWEC. In Proceedings of the European Wave and Tidal Energy Conference, Bilbao, Spain, 3–7 September 2023; Volume 15. [CrossRef]
94. Welcome to Python.org. Available online: https://www.python.org/ (accessed on 3 April 2022).

95. Chiri, H.; Pacheco, M.; Rodríguez, G. Spatial variability of wave energy resources around the Canary Islands. In *WIT Transactions on Ecology and the Environment*; WIT Press: Southampton, UK, 2013; pp. 15–26. ISSN 1743-3541. [CrossRef]
96. JA SOLAR. Harvest the Sunshine: 650 W (JAM72D42 LB). Available online: https://www.jasolar.com/statics/gaiban/pdfh5/pdf.html?file=https://www.jasolar.com/uploadfile/fujian/2024/1120/b1d39cfaeb1d0f5.pdf (accessed on 28 November 2025).
97. Dupont, E.; Koppelaar, R.; Jeanmart, H. Global available solar energy under physical and energy return on investment constraints. *Appl. Energy* **2020**, *257*, 113968. [CrossRef]